HOLOGRAPHIC SCANNING LASER ACOUSTIC MICROSCOPY (HOLOSLAM): A NEW QNDE TOOL

A. C. Wey, and L. W. Kessler

Sonoscan, Inc.
530 E. Green Street
Bensenville, Illinois

INTRODUCTION

Acoustic microscopy is the name given to high frequency, 10 MHz to 3 GHz ultrasonic visualization. The scanning laser acoustic microscopy (SLAM) is an important branch of acoustic microscopy which uses ultrasound in the frequency range of 10 to 200 MHz to produce high resolution ultrasonic images.[1,2] In contrast to other visual observation techniques, SLAM provides direct access to the structural elastic properties of solid materials and biological tissues. By using this technique, valuable insight can be gained into mechanisms responsible for the changes of elastic architecture over areas tens of microns in diameter.

SLAM's principle of operation has been presented and discussed extensively in the literature.[3,4] The technique is based on transmitting ultrasound through the specimen and obtaining a dynamic ripple caused by the ultrasound on a solid mirror-like free surface above the specimen. The resulting image depicts the acoustic transmission properties of the insonified specimen and is obtained by employing a scanning laser beam as a point-by-point detector of ultrasound wave. With laser beam scanning technology, the images are produced in real-time, that is, at conventional TV rates of 30 frames per second.

The variations in ultrasound transmission are displayed on a TV monitor where the bright regions correspond to defect-free areas of high transmission through the sample, whereas, the darker areas correspond to regions of higher ultrasonic attenuation attributed to defects or changes in elastic properties because of scattering, reflection or absorption of ultrasound. Therefore, SLAM allows us to actually see inside objects and locate defects which are not evident at the surface.

SLAM operates in a transmission mode. On the one hand, it can interrogate the entire thickness of the sample in real time. On the other hand, however, SLAM micrograph is a composite shadowgraphic image which contains both in-focus and out-of-focus information. Because of diffraction the resultant images are often unfocused and difficult to comprehend especially

Review of Progress in Quantitative Nondestructive Evaluation, Vol. 9
Edited by D.O. Thompson and D.E. Chimenti
Plenum Press, New York, 1990

when test specimens have substantial thickness. To overcome this difficulty we have modified a conventional SLAM and developed a holographic image processing technique which enables SLAM to focus object in the same fashion as an optical microscope.

In this paper we describe the conversion of a SLAM to a holographic imaging system (HOLOSLAM). The modification of SLAM to acquire data for holographic image reconstruction is discussed. The holographic image processing and velocity imaging algorithms are described. The applications of HOLOSLAM in ND inspection of structural materials are presented.

DATA ACQUISITION FOR HOLOSLAM

In a practical SLAM, a low power laser beam scans the dynamic surface caused by ultrasound wave. A knife-edge technique is employed to visualize the surface perturbation[5]. Fig. 1 shows the knife-edge technique used in SLAM for acoustic signal detection. The laser beam intensity is detected by a knife-edge and photodiode combination whose output is an electronic signal carrying the spatial information of the ultrasound wavefield. The intensity of the scanning laser can provide an amplitude distribution of the ultrasound wavefield. However, to perform holographic reconstruction, phase information must be preserved.

A quadrature receiver was designed for HOLOSLAM to obtain both the amplitude and phase information for holographic reconstruction. Quadrature detection involves multiplying the signal with two coherent electronic references[6]. One reference has its phase shifted by 90 degrees with respect to the other. The schematic diagram of quadrature receiver is shown in Fig. 2. The two outputs represent the real and imaginary parts of the complex amplitude of the ultrasound, respectively, and are given by[6]

$$y_1(x) = -K2\pi f_x A(x)\sin(2\pi f_x x - \psi(x)) \quad (1)$$

$$y_2(x) = K2\pi f_x A(x)\cos(2\pi f_x x - \psi(x)) \quad (2)$$

where f_x is spatial frequency of the surface ripple and K a constant which depends upon the electronic circuit of the system. The amplitude A(x) and phase $\psi(x)$ can be obtained by directly solving equations (1) and (2).

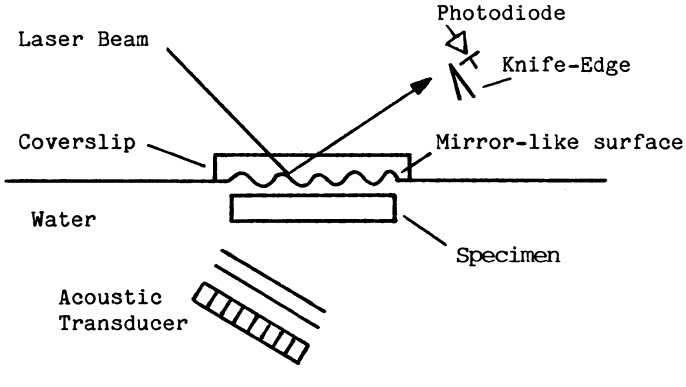

Fig. 1 Knife-edge technique for acoustic signal detection in SLAM.

HOLOGRAPHIC IMAGE RECONSTRUCTION

In SLAM, an ultrasonic plane wave propagates through a test object. Consider an object consisting largely of homogeneous material but with a particular internal plane having a distribution of inhomogenieties. The distribution may consist of defects or a pattern of different materials within the specimen. It is the objective of holographic image reconstruction to image this particular subsurface plane nondestructively.

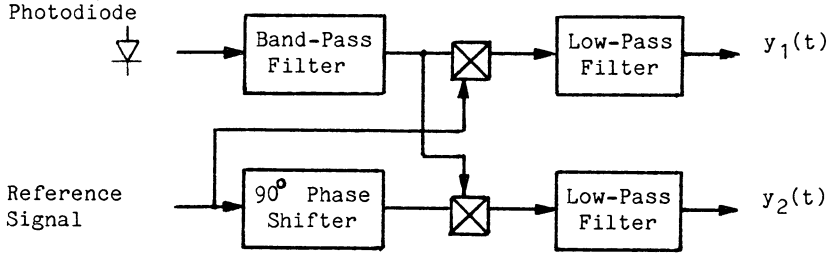

Fig. 2 Block diagram of the electronic circuit for quadrature detection.

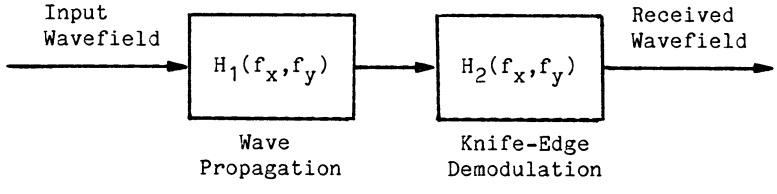

Fig. 3 A linear system model of SLAM imaging process.

The SLAM imaging process can be modeled as a linear system[7] as shown in Fig. 3. The input to the system is the wavefield distribution at the particular plane of interest. The system contains two linear filters. One corresponds to the wave propagation through the homogeneous medium. The other characterizes the response of the knife-edge detection. The transfer functions representing wave propagation and knife-edge detection can be found in the reference[7]. With these transfer functions, it is possible to design inverse filters for the image reconstruction.

The block diagram of the image reconstruction is shown in Fig. 4. The inverse filter for $H_2(f_x,f_y)$ is designed as follows[7]:

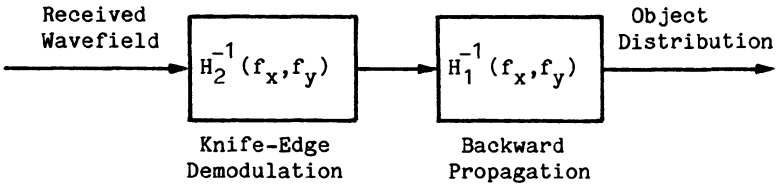

Fig. 4 Inverse filtering model of image reconstruction.

$$H_2^{-1}(f_x,f_y)=\begin{cases}\dfrac{H_{max}\exp\left(\frac{\pi^2 r_o^2}{2}(f_x^2+f_y^2)\right)}{j\,\mathrm{erf}\left(\frac{\pi r_o f_x}{\sqrt{2}}\right)}, & \text{if } |H_2(f_x,f_y)| \geq H_s \\ 1, & \text{otherwise}\end{cases} \quad (3)$$

where H_s is the threshold chosen in such a way that after inverse filtering the main spectrum of the signal is recovered and the noise amplification does not degrade the image reconstruction[7]. H_{max} is the amplitude of the maximum response for $H_2(f_x,f_y)$. Here we assume that the laser beam scans in the x-direction and has a Gaussian intensity profile and an effective beam radius of r_o.

The diffraction experienced by wavefield propagation can be corrected by computing the corresponding backward propagation. The corresponding inverse filter to accomplish this is

$$H_1^{-1}(f_x,f_y) = \begin{cases}\exp\left(-j2\pi z\left(\frac{1}{\lambda^2} - f_x^2 - f_y^2\right)^{\frac{1}{2}}\right), & f_x^2 + f_y^2 \leq \frac{1}{\lambda^2} \\ 0, & \text{otherwise}\end{cases} \quad (4)$$

where λ is the wavelength of the ultrasound within the homogeneous medium, and z the distance between the object plane and receiving plane. With this inverse filtering technique, the corresponding object distribution at a specific depth can be reconstructed from the received wavefield.

The holographic SLAM contains a standard SLAM with modified electronic circuit for quadrature detection and an IBM Personal Computer AT compatible with a 10 MHz 32 bit co-processor board. The control program was written in the C programming language and runs on the 32-bit co-processor which acts as the main computer using the MS-DOS computer as an I/O controller. The outputs of quadrature receiver are digitized by a video-rate frame grabber. The data acquisition algorithm extracts phase and amplitude data from the digitized outputs of quadrature receiver and then uses them to reconstruct a complex wavefield. The backpropagation algorithm digitally back-propagates the wavefield to a specified depth in a matter of seconds.

QUANTITATIVE VELOCITY PROFILE IMAGING

The measurement of sound velocity has been used to nondestructively characterize materials. In the past several techniques were developed for the SLAM to obtain the sound velocity measurements [8,9]. These techniques are based on the shift of the interference lines obtained by operating the SLAM in the interference mode. However, as high resolution imaging is desired to identify defects within a sample, we have developed a velocity imaging technique employing 2-D phase unwrapping algorithm [10].

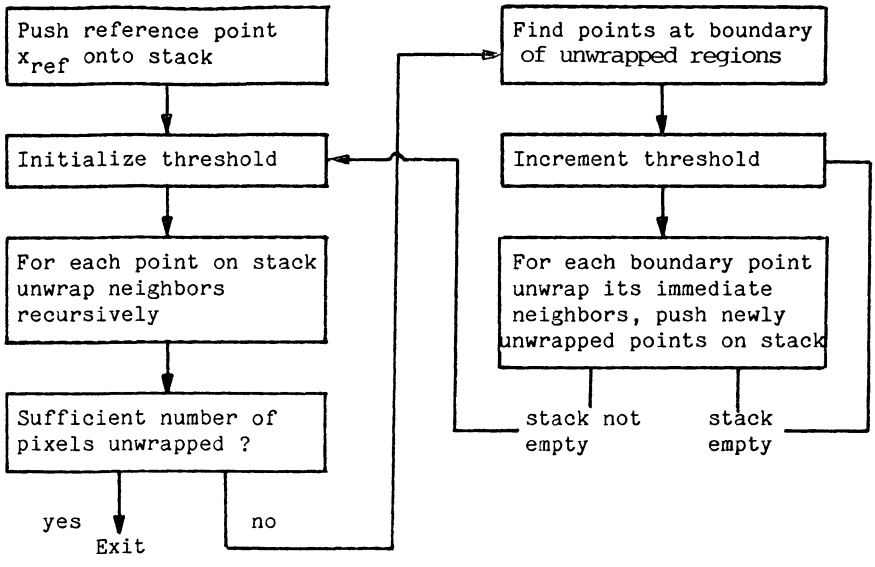

Fig. 5 2-D phase unwrapping algorithm.

Figure 5 shows the flow chart for the 2-D phase unwrapping algorithm. Given a starting location called seed, we unwrap neighboring pixels recursively until no more pixels can be unwrapped. If the number of unwrapped pixels is insufficient, we increment the unwrapping threshold and unwrap only the immediate neighbors of the boundary pixels of the unwrapped region. Any pixels unwrapped here is saved on a stack. After some boundary pixels have been unwrapped, we reset the threshold and repeat the entire process using the pixels on the stack as seeds. The process ends when a sufficient number of pixels have been unwrapped.

The phase successfully unwrapped can be written as

$$\phi u(x) = 2\pi fz\sqrt{1-(c_2(x)\sin\theta_1/c_1)^2}\,/c_2(x) \tag{5}$$

which can be solved for $c_2(x)$ to obtain

$$c_2(x) = 2\pi fz\,/\sqrt{\phi u^2(x)-(2\pi fz\sin\theta_1/c_1)^2} \tag{6}$$

In equations (5) and (6) c_1 and $c_2(x)$ are the velocities for region 1 and 2, and z is the known thickness. The quantities c_1 and θ_1, which is incident angle, are assumed known.

APPLICATIONS AND EXPERIMENTAL RESULTS

It is expected that the power of SLAM could be greatly enhanced through the use of holographic image reconstruction to yield more precise information about the internal features of a given sample. We demonstrated the power of HOLOSLAM by performing 3-D localization of flaws in silicone nitride specimen.

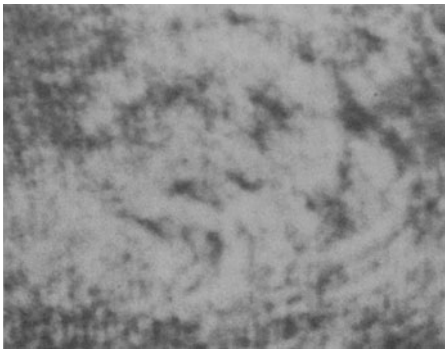

Fig. 6 Typical 100 MHz SLAM micrograph showing diffraction pattern of internal flaws in Si_3N_4 sample.

The thickness of the test specimen was 5 mm. The ultrasound source used in experiments operated at 105.96 MHz, with a field of view 2 mm by 1.87 mm. The specimen was placed parallel to the transducer to assure that only compressional mode propagates through the sample. The compressional mode wave velocity inside the sample was 10,000 m/sec and the velocity of ultrasound in water was 1,500 m/sec. Figure 6 shows a typical SLAM amplitude image which displays diffraction patterns caused by subsurface flaws within the sample. One can easily use SLAM to find flaws by locating this kind of diffraction patterns in SLAM image, but may have difficulty to determine the actual type, shape, size and depth of the flaws.

Fig. 7.a, b, and c show three reconstructed images at depths 0.5, 0.6 and 1.2 mm below the top sample surface, respectively, produced by HOLOSLAM for those defects whose diffraction patterns were shown in Fig. 6. The solid black round spots in Fig. 7.a and b, as pointed by an arrow, indicate voids of 100 um in diameter at 0.5 mm and 0.6 mm depth, respectively. Fig. 7.c reveals a 200 um size inclusion 1.2 mm deep in the sample.

It is interesting to learn that even though a void and an inclusion have almost indistinguishable diffraction pattern in the far field, however, they can be distinguished in the reconstructed HOLOSLAM images where a void completely block the transmission of sound and results in a solid black spot, while an inclusion transmits partially ultrasonic energy and shows a donut-type pattern. Fig. 7.d shows the sketch of a composite view which relates the diffraction patterns in SLAM image as shown in Fig. 6 to the defects found by HOLOSLAM in Fig. 7 a, b and c.

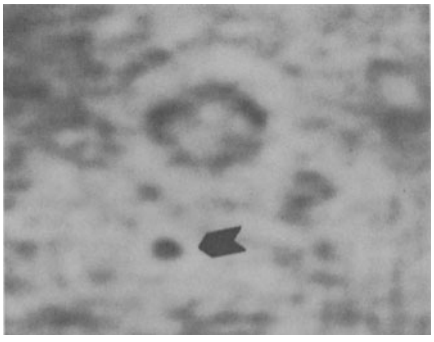

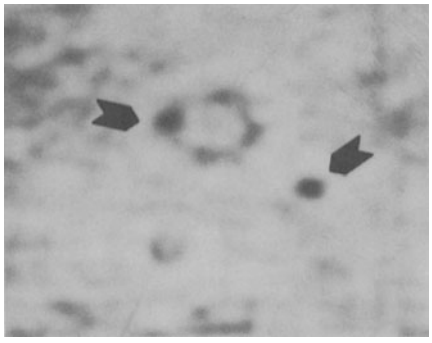

Fig. 7 (a) HOLOSLAM reconstructed image at a depth of 0.50 mm. (b) reconstructed image at 0.60 mm deep.

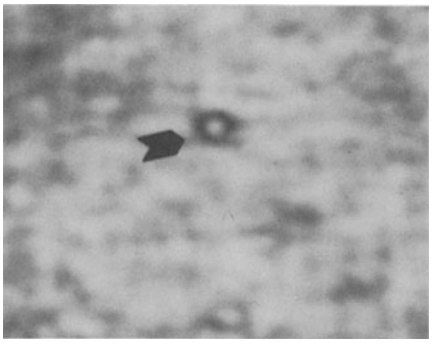

(c) HOLOSLAM reconstructed image at a depth of 1.20 mm.

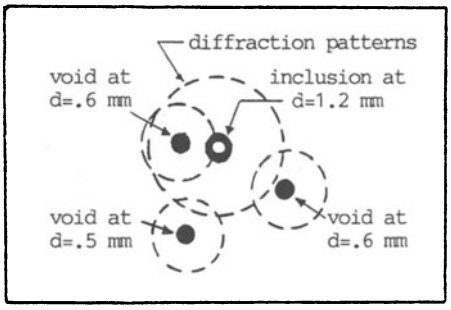

(d) Sketch showing composite view of all defects.

Fig. 7 Reconstructed HOLOSLAM images showing (a) a 80 um void at 0.5 mm deep, (b) two 100 um size void at 0.60 mm, and (c) an 200 um inclusion 1.20 mm deep. The frequency used was 100 MHz with a 2 x 1.87 mm field of view. (d) sketches a composite view of defects-related diffraction patterns as shown in Fig. 6.

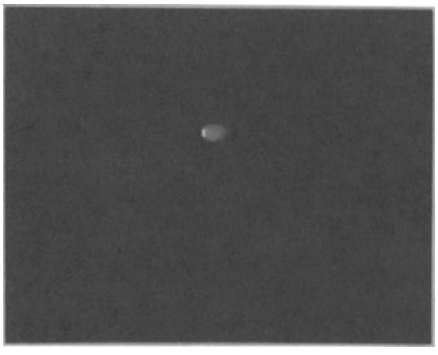

Fig. 8 Computed velocity map for the inclusion shown in Fig. 7.c. The velocity is calculated 8400 m/s which suggests a Si-inclusion. The reference was the measured 10,000 m/s for the host matrix, silicone nitride.

Figure 8 shows a computed velocity map for the image involving the inclusion as shown in Fig. 7.c. The complex amplitude data was saved while conducting holographic reconstruction at a depth of 1.2 mm where the inclusion was located. The phase information was extracted and velocity was then calculated pixel by pixel using the 2-D phase unwrapping algorithm. The inclusion was assumed a spherical one with a measured size of 200 um in diameter. The velocity of the inclusion was estimated about 8400 m/s, in contrast to the host ceramics matrix with a speed of 10,000 m/s. This suggests that the inclusion might be composed of silicone.

SUMMARY

We have reviewed briefly the principles of scanning laser acoustic microscopy (SLAM) and discussed the required modification of a conventional SLAM to become holographic SLAM (HOLOSLAM). Inverse-filtering techniques employed in digital holographic image process are described. Our experimental results show that the wavefield diffraction encountered by regular SLAM can be corrected by holographic image reconstruction. Applications of HOLOSLAM in 3-D localization of flaws in structural materials are presented. The preliminary results from the 2-D phase unwrapping algorithm which provides velocity profile mapping show feasibility using HOLOSLAM to determine the type of flaws within a sample.

ACKNOWLEDGMENT

We would like to thank professor Hua Lee and his student, Richard Chiao at the University of Illinois, Urbana-Champaign for their valuable help in the development of computer algorithms. This work was supported by National Science Foundation under Grant ISI-8604227.

REFERENCES

1. L. W. Kessler and D. E. Yuhas, "Acoustic Microscopy-1979," Proc. IEEE, vol. 67, no. 4, p. 526, 1979.
2. L. W. Kessler, "Acoustic Microscopy Commentary: SLAM and SAM," IEEE Trans. Sonics Ultrason., vol. SU-22, p. 136, 1985.
3. L. W. Kessler and D. E. Yuhas, "Principles and Analytical Capabilities of the Scanning Laser Acoustic Microscopy," Scan. Elec. Microscopy, vol. 1, p. 555, 1978.
4. L. W. Kessler and M. G. Oravecz, "SLAM Analysis of Advanced Materials for Internal Defects and Discontinuities," Proc. of NDT/E of Adv. Mater. and Comp., p.173, 1986.
5. R. L. Whitman, A. Korpel, "Probing of Acoustic Surface Perturbations by Coherent Light," Applied Optics, vol. 8, no. 8, p. 1567, 1969.
6. Z. Lin, H. Lee, G. Wade, M. Oravecz and L. W. Kessler, "Data Acquisition in Tomographic Acoustic Microscopy," Proc. IEEE Ultrasonic Symp., p. 627, 1983.
7. G. Wade and A. Meyyappan, "Scanning Tomographic Acoustic Microscopy: Principles and Recent Developments," SPIE vol. 768, p. 267, 1987.
8. D. R. Grant and J. E. Bernardin, "Measurement of Sound Velocity with the Scanning Laser Acoustic Microscope," J. Acoust. Soc. Am., 69(3), p. 437-444, 1981.
9. P. M. Embree, K. M. Tervola, S. G. Foster, and W. D. O'Brien, Jr., "Spatial Distribution of the Speed of Sound in Biological Materials with the Scanning Laser Acoustic Microscope," IEEE Trans. Sonic Ultrason., vol SU-32, p. 341-350, 1985.
10. R. Y. Chiao and H. Lee, " High Resolution Velocity Images Using the Scanning Laser Acoustic Microscope," Proc. 1988 IEEE Ultrasonic symp.